Ultramicroscopy 8 (1982) 163–174
North-Holland Publishing Company

NEW IMAGING METHODS FOR CATALYST PARTICLES

A. Howie, L. D. Marks and S. J. Pennycook

Cavendish Laboratory, University of Cambridge,
Madingley Road, Cambridge CB3 OHE, England

The application is described of various bright field and dark field imaging methods to the study of catalyst and other small particles in the presence of scattering effects from the support. A major advance has been possible with the use of annular dark field, Z contrast and microdiffraction techniques in the STEM. Microanalysis of individual particles can now be carried out almost routinely. Methods of imaging surface structure are under development and it may also be possible to extract useful information about valence electron properties.

1. INTRODUCTION

For the past twenty years transmission electron microscopy has been the dominant technique for the investigation of microstructure in materials science and metallurgy. Parallel development in the fields of chemistry and industrial catalysis has, however, been delayed by a number of factors. In some cases the structures of interest have much larger unit cells than those of the metallurgist or are more disordered and have had to await the advent of high resolution microscopy and direct structure imaging. In many other instances the more or less complete lack of microanalytical facilities on the conventional transmission microscope was no doubt regarded as a very serious drawback by the typical chemist interested in composition at least as much as in structure. The development by Crewe and co-workers (1) of the scanning transmission electron microscope (STEM), particularly with the high brightness field emission gun, combines the high resolution capability of the conventional machine with the microanalytical facilities offered by scanning techniques and has transformed the situation radically.

Now that the way to further progress seems clear these problems might be regarded entirely as a matter of history but for the fact that they have left the subject in a very uneven state of development providing further reasons for confusion and delay. The industrial chemist, curious about the possible use of transmission electron microscopy, may either stumble forward in relative ignorance encountering many of the pitfalls met by metallurgists many years ago or he can seek enlightenment in the considerable literature existing mostly in unfamiliar journals. There he will find the virtues urged upon him of a bewildering array of sophisticated and interlocking instrumental and imaging techniques, many of which may be of little value for his particular problems. The resolution of these difficulties will require time and quite probably the publication of an appropriate treatise written for his colleagues by a catalyst chemist who has mastered the subject for himself. It would certainly be presumptuous to claim that the present article can do more than point out the difficulties and indicate some promising directions.

Catalysts provide an extreme example of the extent to which the nature of available specimens can dictate the kind of microscopy which is desirable or even possible. High resolution imaging is only one of several conflicting goals and may frequently have to be compromised severely in the search for an optimum solution. In the case of bulk samples for instance, which can generally be easily studied only in the conventional scanning microscope, the resolution is generally limited by multiple scattering and beam spreading effects within the specimen as well as by noise due to inadequate source brightness to figures in excess of 20 nm for structural detail and perhaps several μm for X-ray microanalysis. Nevertheless in situations where a minimum of interference with the real catalyst is essential, the images obtained can often provide at great depth of field a vivid low resolution picture of its structure and even of the dynamics of its operation (2),(3).

For higher resolution it is generally necessary to employ transmission techniques on samples thinned to less than 100 nm or even to less than 10 nm. The various thinning methods currently employed such as crushing and collecting a dispersion of fine particles or ultramicrotomy (possibly after crushing and embedding in epoxy) can clearly lead to serious physical or chemical damage as well as to the risk that non-typical features may be selected. Despite these problems the usefulness of transmission studies in determining catalyst particle sizes and dispositions is well established (3,4,5) and the possibility of observing in-situ catalytic reactions (albeit at only moderate resolution of $\sim$ 2 nm and without facilities for microanalysis) has been brilliantly exploited (6). The development of excellent environmental cells for high voltage microscopes where the electron beam can successfully operate at pressures approaching an atmosphere (7) has enabled these studies to

0304-3991/82/0000–0000/$02.75 © 1982 North-Holland

be extended to a variety of other reactions of catalytic significance (8).

As will emerge below, the typical transmission specimen produced from a real catalyst may still be far from ideal for high resolution work. It may then be judged preferable to study simulated specimens where the particles are produced by evaporation or other means on special pre-thinned substrates chosen for their electron-optical properties. Such specimens may be even further removed from the real catalyst than the sample which has been obtained from it by drastic thinning procedures, though closer to it in some respects than the idealised single crystal surfaces employed in many broad beam investigations like LEED.

Even with these many compromises over specimen treatment, the electron microscopist may well find himself compelled within the limitations of the available equipment to adopt new imaging procedures and techniques of interpretation to extract the information he requires. In the following sections we review the current situation in this respect, starting with the conventional transmission microscope which is still by far the most generally available instrument before going on to deal with the various aspects of the STEM which appear to offer a great range of new opportunities for obtaining high resolution information directly relevant to catalysis.

2 CONVENTIONAL TRANSMISSION ELECTRON MICROSCOPY

2.1 Contrast Mechanisms for Crystalline Specimens

In the conventional microscope inelastic scattering, being concentrated at relatively small energy losses and at scattering angles well within the objective aperture, plays a very minor role in determining image contrast apart from limiting the maximum specimen thickness for high resolution studies via its contribution to spatial and temporal incoherence. The main contrast effects arise from elastic scattering which gives amplitude contrast (sometimes called diffraction contrast) when the angle exceeds the objective aperture semi-angle. Phase contrast effects arise when larger objective apertures are used with semi-angles exceeding the scattering angle. For crystalline supports and all but the smallest catalyst particles, the elastic scattering is due to Bragg reflection and we can refer to the simplified but qualitatively useful dynamical theory expression for the intensity of diffraction from planes of spacing d in a crystal of thickness t misoriented by $\Delta\theta$ from the exact Bragg position (9)

$$I_B = \sin^2(\pi t\sqrt{1 + w^2}/\xi_g)/(1 + w^2) \qquad (1)$$

where $w = \xi_g \Delta\theta/d$ and ξ_g is the extinction distance for the Bragg planes used (typically lying between 20 nm and 50 nm for low order reflections). Clearly the diffracted intensity can be comparable to unity for small $\Delta\theta$ values, giving rise to strong contrast effects with, however, a sharp dependence on specimen orientation relative to the electron beam. The dangers of confusing such orientation effects with genuine differences in particle thickness or shape have been pointed out (10,11).

A secondary contrast mechanism arises from incoherent, quasi elastic scattering mainly due to thermal diffuse scattering outside the objective aperture. In the case of a thin crystal an approximate expression for the total diffuse intensity is

$$I_D = \frac{t}{V_a}(1 + F)\int \frac{d\sigma}{d\Omega}(1 - e^{-2M(\theta)})d\Omega \qquad (2)$$

where $d\sigma/d\Omega$ is the differential atomic scattering cross section, $M(\theta)$ the Debye Waller constant and V_a the atomic volume. The function F describes variations in I_D due to channelling effects and depends on the incident beam orientation as well as on crystal thickness. Typically the maximum channelling effect occurs for $t \approx 5$ nm for 80 keV electrons where F can vary between - 0.5 and perhaps + 3.0 for different orientations. A fuller and more accurate account of these effects can be found in (9).

2.2 Diffraction Contrast Imaging Methods

Although axial bright field imaging is probably still the most widely used diffraction contrast technique in catalyst studies, there are a number of dark field methods which can offer advantages in detecting small particles and in assessing their structure and shape. Conventional dark field imaging, where the illumination is tilted so that the objective aperture can remain on axis and accept a small portion of a diffraction ring arising from the particles was employed (4) for instance to show that the fraction of multiply twinned particles (MTP) in a number of Ni, Au, Pt and Pd catalysts was extremely small. More recently, substantial numbers of MTP, sometimes in the form of quite large particles, have been found in Ag catalysts (12). Figures 1(a) and (b) show bright field and dark field images of these structures in evaporated silver particles and make clear the superiority of the dark field image for selecting and identifying the differently oriented crystal segments.

The lack of azimuthal symmetry in conventional dark field imaging implies a directional selectivity in scattering and possibly also astigmatic problems at high resolution which could be disadvantageous. More sophisticated axial techniques were originally developed for identification of small particles in epitaxy studies and employed either an annular objective aperture (13) or an annular condenser

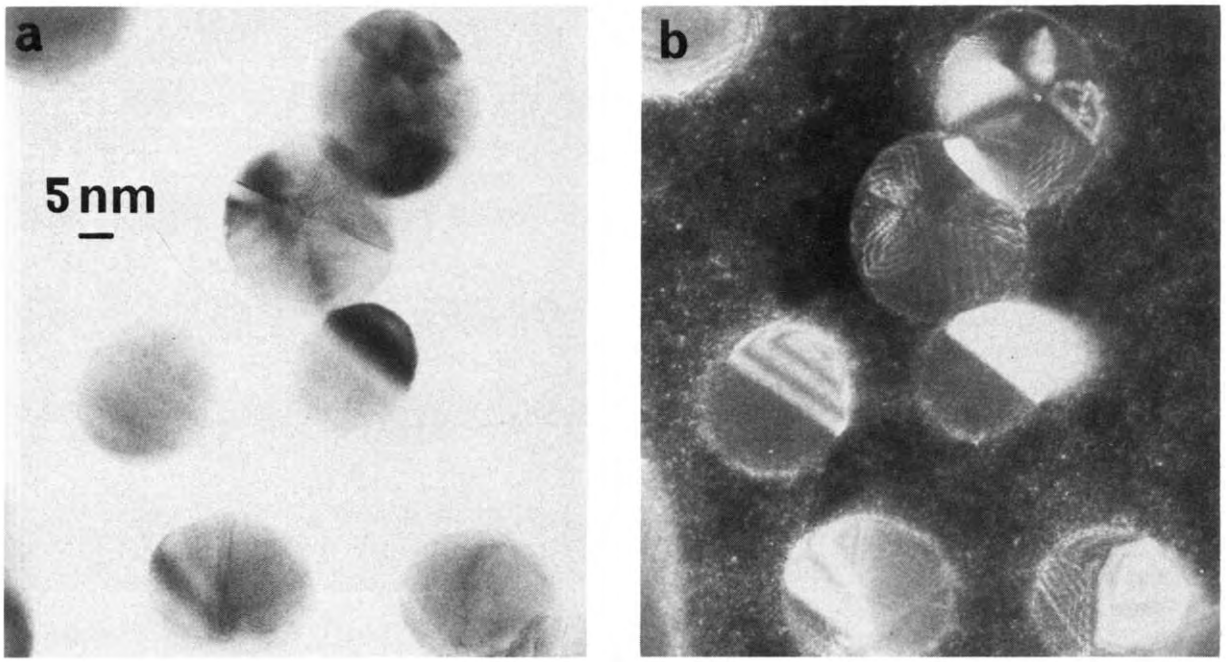

Fig. 1 Multiply-twinned particles of evaporated silver. The different crystal segments and thickness fringes are more visible in dark field (b) than in bright field (a).

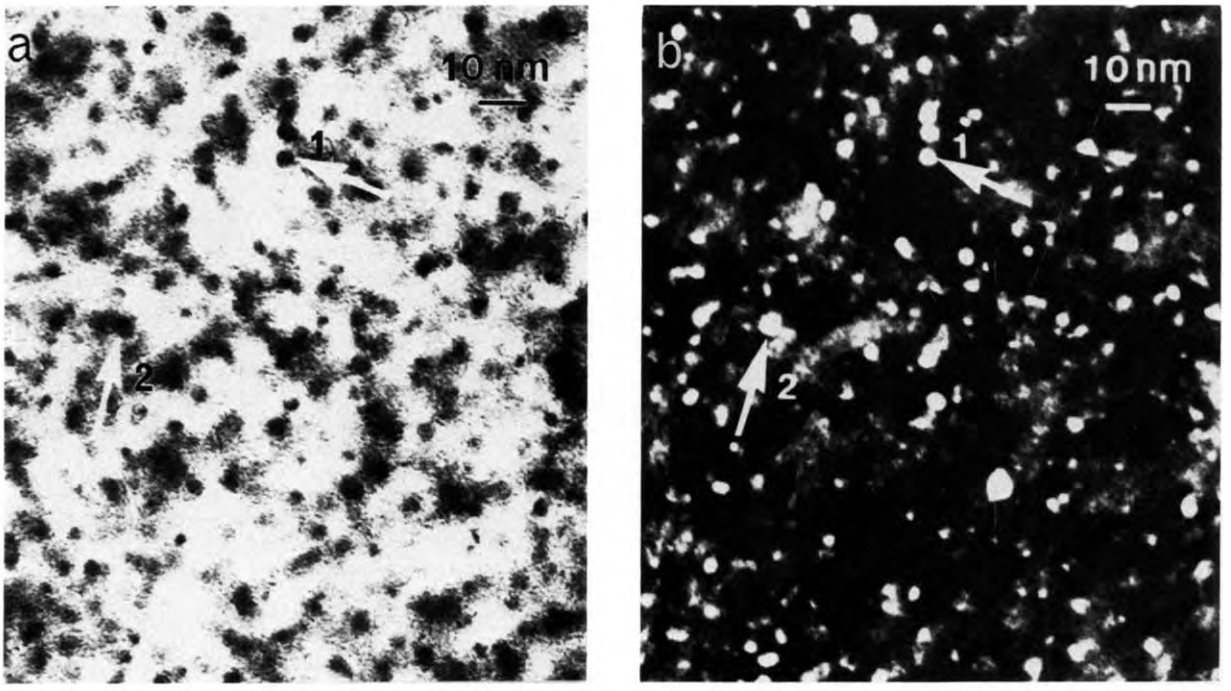

Fig. 2 Pd particles on γAl_2O_3 support imaged in axial bright field (a) and dark field hollow cone illumination (b).(15)

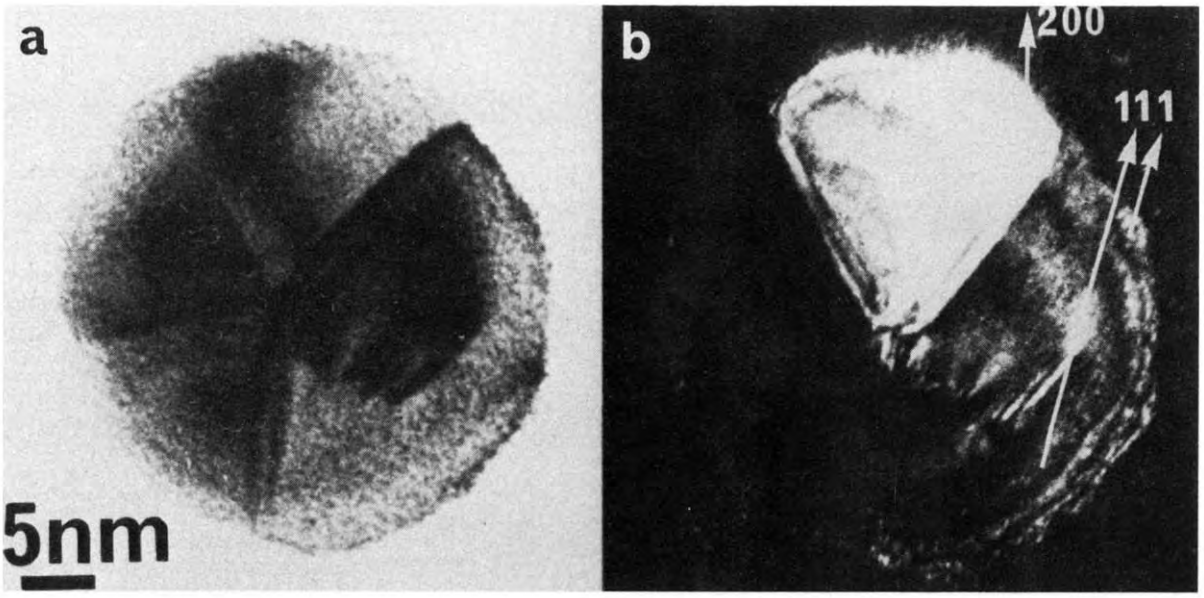

Fig. 3 Decahedral particle of evaporated silver imaged in bright field (a) and dark field (b) showing internal defects, surface facets and notches. The diffraction spots contributing to the dark field image are indicated in (b).

aperture (14) allowing in each case a selected zone of scattering angles to be accepted. The second of these techniques, involving hollow cone illumination, is much easier to put into execution and its usefulness in dark field catalyst studies was demonstrated (15) using a z-stage which allowed the scattering angle selected to be varied without the need to change the annular aperture. An example of this work is shown in figs. 2(a) and (b) where the considerable improvement in visibility of small particles in the dark field hollow cone image can be seen, together with a decrease of the crystallographic contrast of the support.

The selection of particular diffraction conditions, as in the conventional dark field image fig. 1(b), can be very useful when the object is to characterise a few particles as accurately as possible rather than to detect all of them. Many of the diffracting segments evidently exhibit thickness fringes of the type predicted by eqn.(1) with a periodicity $\Delta t = \xi_g/\sqrt{1 + w^2}$. Particularly if a large value of w, the deviation from the Bragg position is employed, these fringes can be used to profile with fair accuracy the shape of the particle, identifying the various facets (16). This is basically an application of the well known weak-beam dark field method (17) employed in electron microscopy to obtain higher resolution diffraction contrast images of defects as well as to detect thickness changes. The method has been used, with very large values of w, to detect monatomic surface steps in very thin gold films (18) and it would certainly be impressive to obtain the same depth sensitivity on catalyst particles. The chief difficulty, indicated by eqn.(1), is that large values of w mean very low intensities I_B which might be submerged in the signal from the catalyst support.

The weak beam technique is also potentially useful when catalyst particles contain crystal defects such as dislocations which occur in some of the MTP.

The defect images obtained can be much sharper than in bright field or in strong beam dark field ($w \approx 0$) and an example is shown in fig.3. Setting up sufficiently precise weak beam diffraction conditions in individual particles is not always easy but one solution is to obtain first the situation of a strong dark field intensity, with tilted illumination θ, and then to change the illumination tilt to $-\theta$.

2.3 High Resolution Direct Structural Imaging

The direct imaging of structure by high resolution axial bright field methods is now one of the most active branches of electron microscopy. Although catalysts are generally far from ideal objects for such work, useful images (correlating with catalyst properties) have been

obtained in the case of $LaPO_4$ catalysts (19) and Ni-Mo-O catalysts (20). The fine structure of supports like graphitised channel black (21) can readily be imaged and the disposition of Pt catalyst particles upon it. However it is rather difficult to image the particle structure directly, partly because the lattice spacings involved are near the limits of resolution and possibly also because scattering in the support may destroy the phase contrast. This dephasing effect could be particularly serious for particles on the beam entrance side of the support since the different diffracted beams from the particle then explore different regions of the support and experience different phase shifts.

At higher voltages resolution can be improved and possible dephasing effects from the support are reduced because of smaller diffraction angles. Figure 4 shows an image of a Pt-graphite intercalate (22) and fig. 5 one of an Ag icosahedral MTP (23) viewed along the [112] direction, both taken on the Cambridge high voltage, high resolution microscope. In the case of the Ag particle, the extra penetration of the 500 keV electrons is a useful additional factor. Structural images of MTP (23) have demonstrated the presence of internal dislocations (arrowed in fig. 5) as well as identifying directly the various constituents of a variety of poly-particles formed by the coalescence of different MTP. These studies also highlight the difficulties caused by overlap effects when axial bright field imaging is applied to objects with complex 3-dimensional structure.

The problem of overlapping effects in electron microscopy occurs because, even in high resolution imaging, the objective aperture accepts only a rather small range of scattering angles and the image is therefore derived from a two-dimensional projection of the object structure. The consequent problems of structural interpretation become increasingly severe for more highly disordered structures and culminate in the severe statistical overlap problem which arises in electron microscopy of amorphous materials (24). Chance alignments of atoms along the beam direction give rise to a characteristic fringey structure in bright field and it can be very difficult to distinguish the presence of small clusters against the background noise from the support even when there is a substantial difference in atomic number between cluster and support (11). Figures 6(a), (b) and (c) show the situation in bright field at various defocus values. Similar problems occur in the conventional dark field image shown in fig. 6(d) where the statistical effects from the support give rise to a speckle pattern of bright spots of diameter equal to the instrumental resolution which cannot readily be distinguished from small clusters. The situation is transformed in hollow cone dark field imaging, fig. 6(e), where the effects due to purely statistical alignments over the thickness of the support are largely washed out. This arises from the use of an annular illumination aperture with a semi-angle much greater than the objective aperture semi-angle and a correspondingly large range of scattering angles. An approximate theory of incoherent hollow cone dark field imaging has been

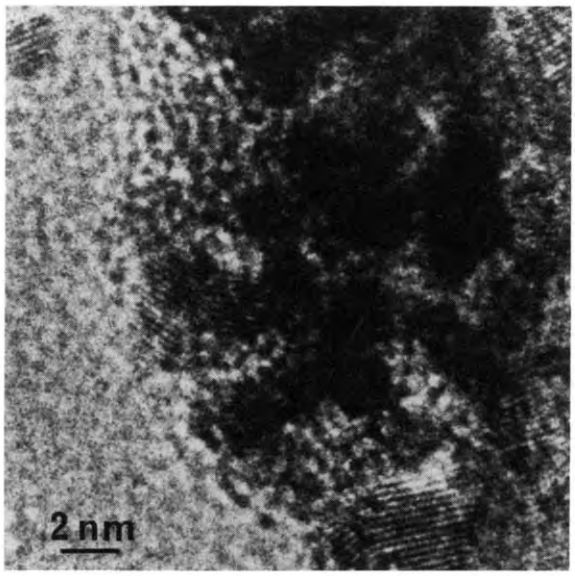

Fig. 4 High resolution axial bright field image of a Pt-graphimet particle (22).

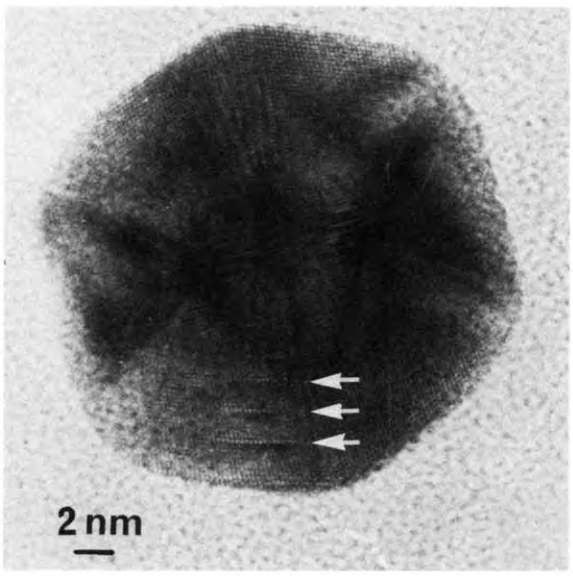

Fig. 5 High resolution axial bright field image of a silver icosahedron (23) viewed along [112]. Dislocations are arrowed.

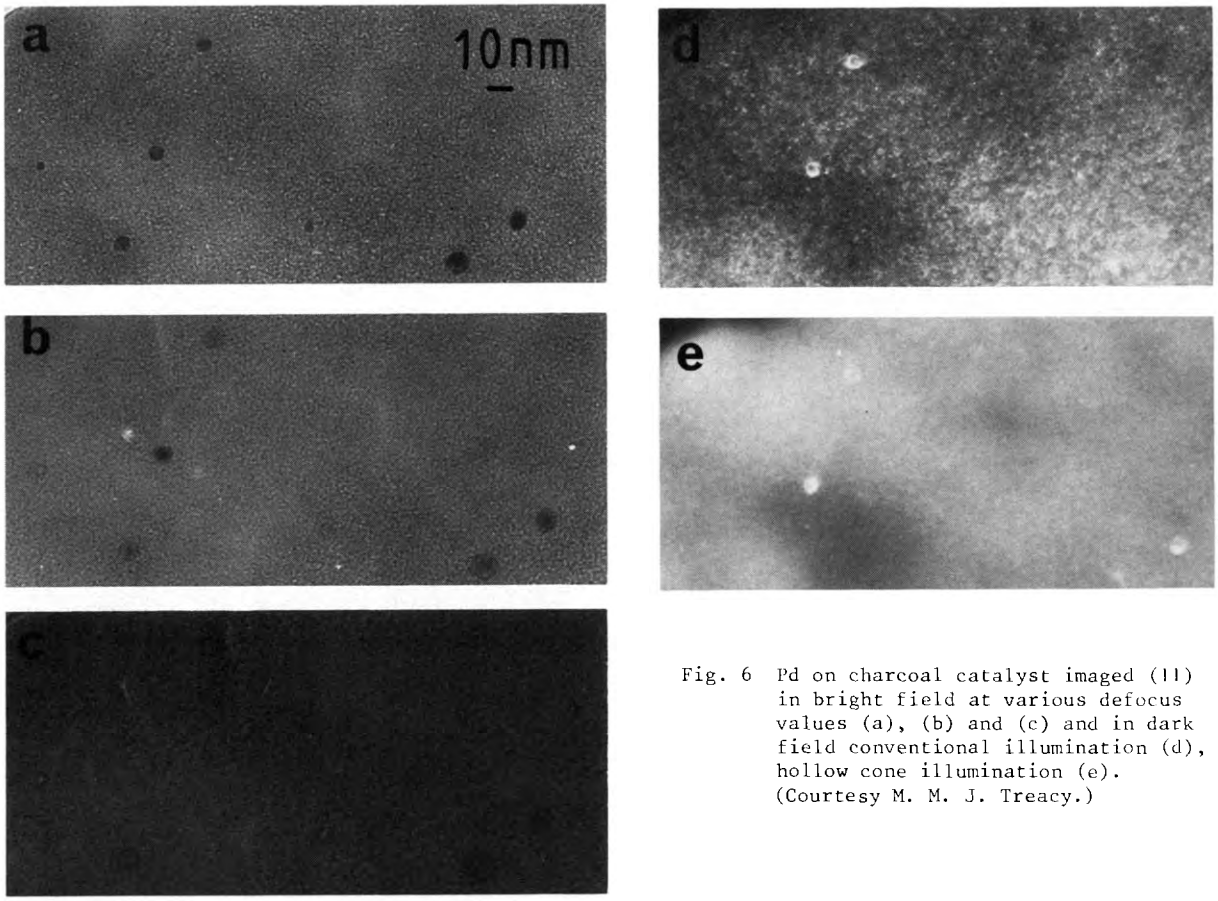

Fig. 6 Pd on charcoal catalyst imaged (11) in bright field at various defocus values (a), (b) and (c) and in dark field conventional illumination (d), hollow cone illumination (e). (Courtesy M. M. J. Treacy.)

developed to explain these effects (25). The use of incoherent illumination has also been tried in bright field (26) and seems again to give some improvement in the visibility of small crystals on an amorphous support.

3 SCANNING TRANSMISSION ELECTRON MICROSCOPY

3.1 STEM Imaging Modes

STEM images are derived from a variety of signals generated when an electron beam focused to a fine (< 1 nm diameter) probe is scanned across the specimen. STEM attachments are available for conventional microscopes but the full potential of the method certainly cannot be attained unless a field emission source is employed.

Several of the imaging modes which utilise the transmitted electrons can be quantitatively related to familiar modes in the conventional machine by invoking the reciprocity or reversibility principle (27,28). Thus the signal derived from a small aperture axial detector is similar to bright field imaging with a small illuminating aperture and the signal provided by an annular detector is similar to hollow cone dark field imaging. In practice, however, the STEM images are much more powerful since the axial detector is usually placed after an energy spectrometer so that arbitrary energy loss windows can be selected and the annular detector lies at a much larger angle than can be achieved in conventional hollow cone imaging. At the highest angles, $\lesssim$ 100 mrad, the Debye Waller factor greatly reduces the coherent diffracted intensity I_B(eqn.(1)) and the signal comes mainly from the incoherent diffuse intensity I_D (eqn.(2)) which depends mainly on the atomic scattering cross section and displays only the rather weak crystallographic effect due to channelling. This means that the annular detector signal is particularly sensitive to heavy atoms which can deflect the electrons through fairly large angles by Rutherford scattering.

A particularly impressive imaging technique called Z contrast was developed by Crewe et al.(1) for imaging individual heavy atoms on extremely thin light atom supports. The annular detector signal and the axial detector signal corresponding to about 20 eV energy loss are collected simultaneously and an image displayed corresponding to either the ratio or the difference of the two signals. This procedure tends to cancel out confusing image

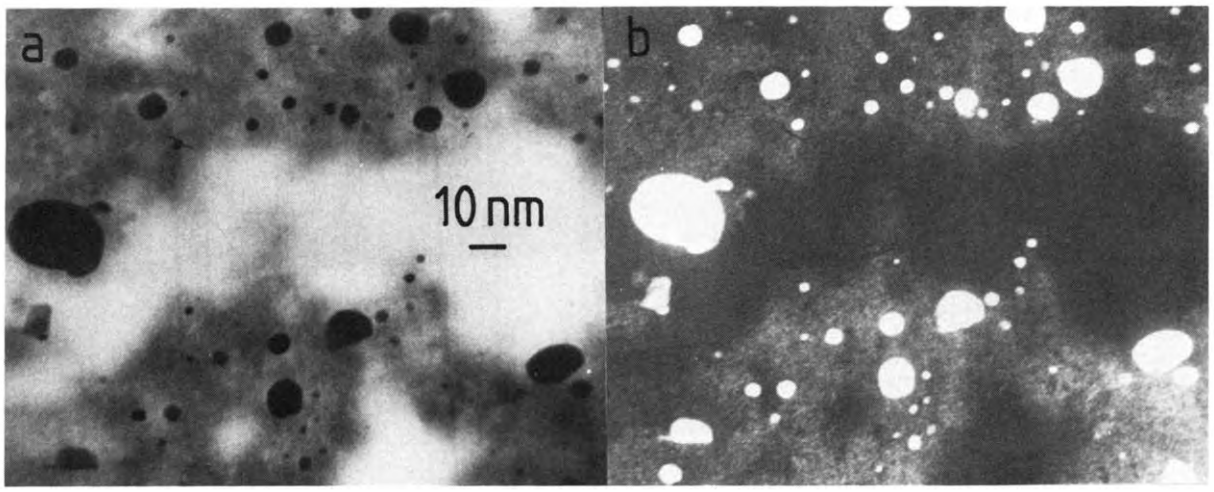

Fig. 7 STEM images of Pd on charcoal catalyst (courtesy M. M. J. Treacy), showing bright field zero loss in (a), Z contrast ratio image in (b).

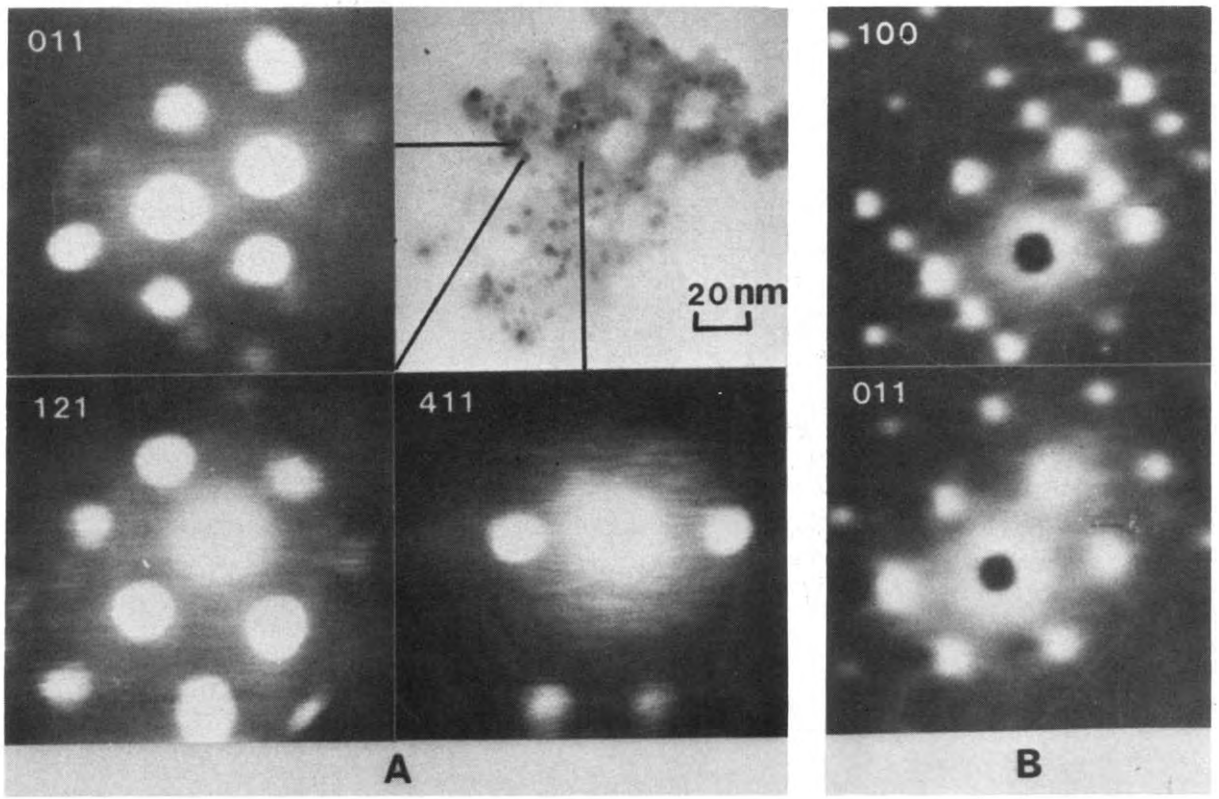

Fig. 8 Microdiffraction patterns taken from individual Ru catalyst particles: (a) Courtesy Journal of Microscopy (31). The better quality patterns (b) were obtained with an optical recovery system (33), courtesy J. Butler.

detail due to variations in the thickness of the support or to fluctuations in the source intensity so that the visibility of the individual heavy atoms is greatly improved.

The Z contrast method was also found (29) to give improved visibility of many small catalyst particles in specimens produced from real catalysts with supports whose thickness is inevitably considerably greater. Figure 7 shows an example for Pd on charcoal. The observations were made with an annular detector covering the range 13 to 50 mrad however and appreciable coherent Bragg scattering effects were observed both from the particles and from crystalline regions of the support. In such a situation coherent diffraction produces complementary signals in the annular detector and energy loss detector so that the effect can be accentuated by taking the ratio or difference. Later experiments comparing the signals from this annular detector with a second one built into the specimen cartridge and covering the range 100 mrad to 400 mrad, showed (30,31) that the signal from the second, high-angle, detector was much less sensitive to coherent scattering effects and depended on crystal orientation only because of the channelling effect mentioned in Section 2.1. The signal from this detector was adequate on its own and was not improved by taking the ratio or difference with the energy loss signal.

Recent observations (32) of very small clusters of a number of different atoms on very thin carbon supports have suggested that they are in a state of dynamic equilibrium with their structures constantly changing and atoms frequently escaping to transfer to another cluster. If, as is argued, these effects are genuinely a consequence of thermal agitation and not stimulated by either knock-on or electronic excitation from the electron beam, the observation is clearly an extremely significant one.

Microdiffraction patterns can be obtained very effectively in the STEM with the focused probe stopped on a catalyst particle. Figure 8(a) shows a number of these patterns taken (31) from a catalyst of Ru on SiO_2 which clearly demonstrate the single crystal nature of the particles and indeed indicate that they have effectively the bulk structure. These patterns were generated by post-specimen scanning of the scattered electrons over the axial detector while the probe was stopped on each particle. Much more efficient equipment (33), kindly made available to us by Professor Cowley, allows the diffraction pattern to be recorded optically from a fluorescent screen yielding in a fraction of a second the better quality patterns shown in fig. 8(b).

3.2 STEM Microanalysis techniques

By accurate measurements of image intensity levels for heavy atoms in extremely thin supports, the Z contrast technique is capable of providing a considerable degree of discrimination at the atomic level (32,34). Microanalysis techniques based on characteristic X-ray production or electron energy loss spectroscopy have however so far proved more useful for typical catalyst samples. More complete accounts of both these techniques can be found in other contributions to this collection.

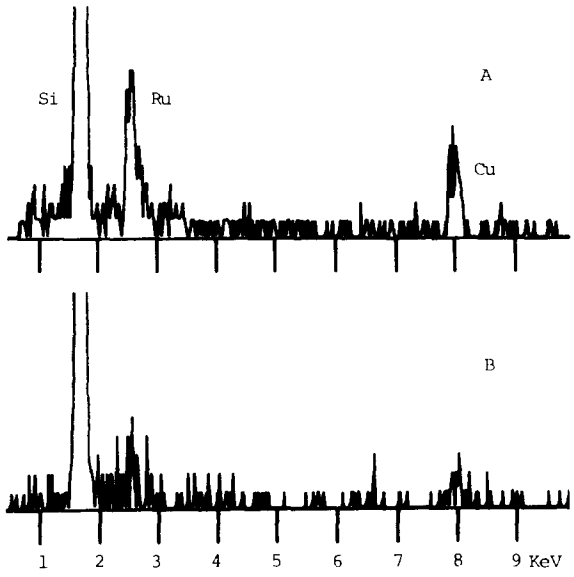

Fig. 9 X-ray spectra from Ru/SiO_2 catalyst (31). (a) Beam on 3 nm Ru particle, (b) beam displaced 3 nm from particle.

Figure 9(a) shows for example the X-ray spectrum recorded (31) from a 3 nm Ru particle on a silica support. Figure 9(b) gives the result when the probe is displaced just to one side of the particle and shows the disappearance of not only the Ru peak but also the Cu peak generated in the specimen grid by stray electrons scattered by the Ru particle. Spreading of the incident electron beam by scattering in fact represents a significant limitation on the localisation which can be achieved in X-ray microanalysis. It would be difficult, for instance, on the basis of X-ray analysis to rule out the existence of a monolayer of Ru covering the whole support (31). Although the initial ionisation occurs via a Coulomb interaction, it is itself quite a localised process even on the scale of the unit cell, since significant contributions to it come from scattering angles greater than the Bragg angle. This means that, rather like the diffuse scattering noted earlier, X-ray production in thin crystals can show an appreciable dependence on orientation relative to the Bragg position because of channelling of the fast electrons (9). Quantitative X-ray data in STEM can easily be upset by this effect if care is not taken to avoid strong Bragg reflections. In the latest STEM models it has been possible to

collect X-ray spectra from 1.5 nm Pt-Rh catalyst particles (35).

Electron energy loss spectroscopy (EELS) is based like X-ray microanalysis on the ionisation of the core levels of the atom which can be identified by characteristic absorption edges in the loss spectrum in the range up to ∿ 2 keV. Although L, M and higher shells can give useable losses, the best results are usually obtained with K shell losses of light elements and L shell losses from first row transition elements which have a sharp edge structure. In general the method is complementary to X-ray microanalysis. Figure 10 shows the electron energy loss spectrum obtained (31) from a 3 nm Ru particle and fig. 11 that from a 5 nm Fe 'graphimet' particle which turned out to contain oxygen bound as Fe_3O_4 (36).

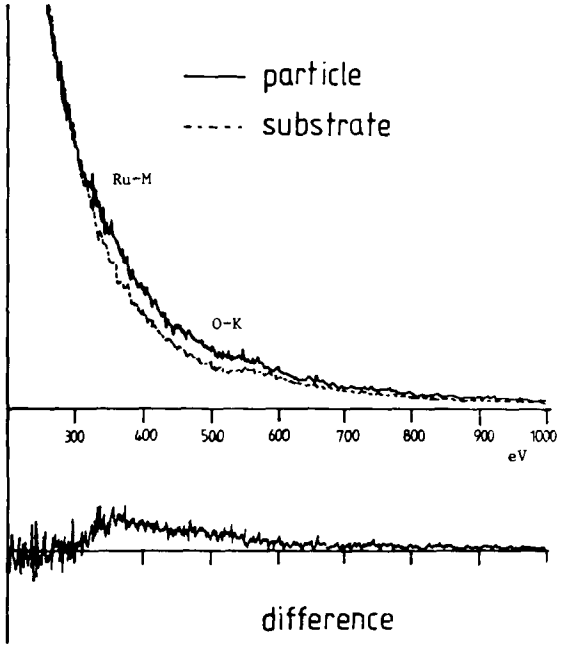

Fig. 10 Electron energy loss spectra from a 3 nm Ru catalyst particle and SiO_2 support. (Courtesy Journal of Microscopy (31)).

The scattering angles accepted in electron energy loss spectra usually correspond to momentum transfers less than a reciprocal lattice vector so that the localisation is usually slightly greater than the lattice spacings. This is adequate for quite high resolution microanalysis but means that complications from channelling effects can generally be avoided. A further advantage of the EELS technique is that it is much less affected by beam spreading effects than the X-ray signal because the spectrometer generally rejects electrons which have been scattered through more than quite small angles.

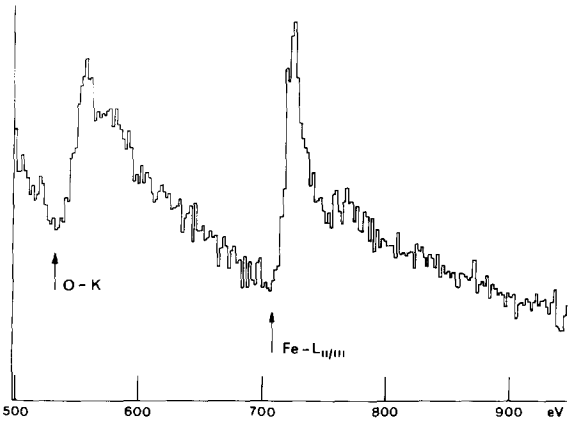

Fig. 11 Electron energy loss spectrum from a 5 nm Fe graphimet particle protruding over the edge of the graphite support.

The combination of EELS, X-ray spectroscopy and microdiffraction is a very powerful one for studying individual small catalyst particles and can now be carried out almost routinely. The spectra can be acquired simultaneously and at the same time the particle position can be monitored by using the annular detector image so that drift can be eliminated (31).

3.3 Characterisation of Surface Structure and Chemical Properties

Despite the progress which has been made in developing methods for making catalyst particles more visible and for determining their size, shape and composition, electron microscopists are still unable to answer detailed questions about their surface structure and chemical properties. Several other features of the electron energy loss spectrum which could perhaps be useful for this are the low energy region associated with valence band excitations, the fine-structure of the absorption edge region or the EXAFS-like oscillations above the absorption edge. These have all been the subject of some investigation in connection with thin films but only the first has been studied for small particles.

The probability of valence band excitation is quite high but the process is not very localised. Both bulk and surface plasmons can be detected in small particles in the STEM (37) and it is clear that surface plasmon excitation at least can occur when the probe is at some distance from the particle. Marks (private communication) has studied the energy loss spectrum from MgO smoke cubes with the probe directed parallel to one of the faces and at varying distances from it. In the case of a

100 nm cube, the probability of excitation becomes quite significant at distances of 5 nm and multiple excitation has to be considered. It is probable therefore that surface plasmon and possibly other valence excitations of individual particles can be detected but it is not yet clear how sensitive these are to the properties of eventual interest.

Glancing angle diffraction has a long tradition as a surface sensitive technique and has recently been used (38) to spectacular effect in electron microscopy to image the surface steps, emerging dislocations and the nucleation of surface reconstructions in Si crystals. It is much more difficult to apply this technique to small particles but some surface defects have been imaged and a variety of interesting effects observed (39) in the diffraction fine structure of MgO cubes as a result of the interaction of Laue (transmission diffraction) and Bragg (glancing angle diffraction) effects. Since inelastic scattering effects are probably quite strong in all these situations the energy spectroscopy capability of the STEM is likely to be essential in analysing the phenomena.

An alternative technique, related to the idea of low loss scanning microscopy (40), is to tilt the specimen at between 30° and 60° to the incident beam and use the field of the objective lens to focus on to the annular detector the electrons which have been scattered through angles of say 30°. (Some preliminary images of this kind (41) show a minimum resolution of about 5 nm with very little of the foreshortening effect which is a nuisance in glancing angle images.

Strictly speaking, low loss microscopy requires the use of some energy filter to select only those electrons which have lost, say, 200 eV or less. The technique has been used recently (42) in conjunction with a field emission source to image surface structure and defects within about 100 nm of the surface of bulk crystals scanned at incidence angles of $\sim 45^{\circ}$ and with a resolution of perhaps 5 nm. The technique is sensitive to Rutherford scattering and might therefore be of considerable value in imaging bulk catalyst samples.

Secondary electrons could also be used to form STEM images and surface composition could be analysed by Auger spectroscopy. Calculations indicate that there should be enough current to provide a useful Auger signal with a ~ 2 nm diameter electron probe. The degree of localisation which can be expected in the Auger signal is not yet clear however, since multiple scattering and cascade processes can play a role in such low exergy excitations. A useful review of the various problems involved in applying electron microscopy to surfaces is given by Venables (43); see also the paper by Broers in this volume.

We may conclude that the present situation in the application of electron microscopy to catalyst particle characterisation is a very interesting one. Within the constraints of specimen damage which may occur in preparation as well as during examination under the electron beam, existing techniques of imaging and microanalysis are capable of providing a great deal of new information about the structure of real catalysts. A number of imaging methods are potentially useful in providing high resolution structural information about the particles and their structures when scattering from the support is significant. The highly coherent axial imaging techniques which represent the mainstream development in conventional electron microscopy may prove to be less useful in cases where genuine 3-dimensional structure is involved however than the incoherent annular dark field methods of STEM. A number of other STEM imaging modes, particularly those involving energy loss spectroscopy may give useful information about valence electron properties.

We are grateful to Drs. D. J. Smith and M. M. J. Treacy for supplying pictures. The Science Research Council has financed some of this work in conjunction with I.C.I. Ltd. as well as providing support for L.D.M. and S.J.P.

REFERENCES

1. Crewe, A. V., Langmore, J. P. and Isaacson, M. S., Resolution and Contrast in the STEM, in Siegel B. M. and Beaman, D. R. (eds.) *Physical Aspects of Electron Microscopy and Microbeam Analysis* (J. Wiley, New York 1975)

2. Fisher, R. M. and Szirmae, A., Electron Microscope Observations of Iron Catalysed Casification of Graphite in Sturgess J. M. (ed.), *Electron Microscopy 1978* (Electron Microscopical Soc. of Canada, Toronto, 1978)

3. Acres, G. J. K., Bird, A. J., Jenkins, J. W. and King, F. Catalyst Characterisation: Present Industrial Practice in Thomas, J. M. and Lambert, R. M. (eds.) *Characterisation of Catalysts* (J. Wiley, New York 1980)

4. Avery, N. R. and Sanders, J. V., Structure of Metallic Particles in Dispersed Catalysts, J. Catal. 18(1) (1970) 129-32

5. Pope, E., Smith, W. L., Eastlake, M. J. and Moss, R. L., The Structure and Activity of Supported Metal Catalysts, J. Catal. 22 (1971) 72-84

6. Baker, R. T. K. and Waite, R. J., Carbonaceous Deposits from Acetylene, J. Catal. 37 (1975) 101-105

7. Flower. H. M., Tighe, N. J. and Swann, P. R. Environmental Gas Reaction Cells, in Swann, P. R., Humphreys, C. J. and Goringe, M. J. (eds.) *High Voltage Electron Microscopy* (Academic Press, London 1974)

8. Gai, P. L. and Goringe, M. J., Applications of *in situ* Electron Microscopy in Catalysis, in *EMSA Proceedings* (Claitors, Baton Rouge 1981)

9. Hirsch, P. B., Howie, A., Nicholson, R. B., Pashley, D. W. and Whelan, M. J., *Electron Microscopy of Thin Crystals* (Krieger, New York 1977)

10. Flynn, P. C., Wanke, S. E. and Turner, P. S. TEM Studies of Supported Metal Catalysts, J. Catal. 22 (1974) 233-248

11. Treacy, M. M. J. and Howie, A., Contrast Effects in the Transmission Electron Microscopy of Supported Crystalline Catalyst Particles, J. Catal. 63 (1980) 265-269

12. Marks, L. D. and Howie, A., Multiply-twinned Particles in Silver Catalysts, Nature 282 (1979) 196-198

13. Heinemann, K. and Poppa, H., Selected-zone dark field microscopy, Appl. Phys. Lett. 20 (1972) 122-125

14. Heinemann, K. and Poppa, H., High resolution images of crystal lattice planes using conical illumination, Appl. Phys. Lett. 16 (1970) 515-516

15. Freeman, L. A., Howie, A. and Treacy, M. M. J., Bright field and hollow cone dark field electron microscopy of palladium catalysts, J. Microsc. 111 (1977) 165-178

16. Yacaman, M. J. and Ocana, T., High-resolution dark field electron microscopy of small metal particles, Phys. Stat. Sol. (a) 42 (1977) 571-577

17. Cockayne, D. J. H., Ray, I. L. F. and Whelan, M. J., Investigation of dislocation strain fields from use of weak beams, Phil. Mag. 10 (1969) 1265-1270

18. Cherns, D., Direct resolution of surface steps by electron microscopy, Phil. Mag. 30 (1974) 549-556

19. Cowley, J. M., Wheatley, J. C. and Kehl, W. L., High resolution electron microscopy of $LaPO_4$ catalysts, J. Catal. 56 (1979) 185-194

20. Sandars, J. V., High resolution electron microscopy of some catalytic particles, Chemica Scripta 14 (1979) 141-145

21. Millward, G. R., Examination of carbon-supported catalysts by electron microscopy, J. Catal. 64 (1980) 381-396

22. Smith, D. J., Fisher, R. M. and Freeman, L. A., High resolution electron microscopy of graphimets (submitted to J. Catal.)

23. Marks, L. D. and Smith, J. D., High resolution studies of small particles of gold and silver, J. Cryst. Growth 54 (1981) 425-432

24. Howie, A., High resolution electron microscopy of amorphous thin films, J. Non-Cryst. Solids 31 (1978) 41-55

25. Gibson, J. M. and Howie, A., Electron microscopy of amorphous solids, Chem. Scripta 14 (1979) 109-116

26. Nagata, F., Matsuda, T., Komoda, T. and Hama, K., Incoherent illumination method with conventional electron microscope, in Sturgess, J. M. (ed.) *Electron Microscopy 1978* (Electron Microscopical Soc. of Canada, Toronto 1978)

27. Cowley, J. M., Image contrast in STEM, Appl. Phys. Lett. 15 (1969) 58-59

28. Zeitler, E. and Thomson, M. G. R., Scanning Transmission Electron Microscopy, Optik 31 (1970) 258-280

29. Treacy, M. M. J., Howie, A. and Wilson, C. J., Z contrast of platinum and palladium catalysts, Phil. Mag. A38 (1978) 569-585

30. Treacy, M. M. J., Howie, A. and Pennycook, S. J., Z contrast of supported catalyst particles in the STEM, in Mulvey, T. (ed.) *Electron Microscopy and Analysis 1979* (Inst. of Physics, London 1980) pp 261-264

31. Pennycook, S. J., Study of supported ruthenium catalysts by STEM, J. Microsc. 124 (1981) to appear

32. Crewe, A. V., Direct imaging of single atoms and molecules using the STEM, Chem. Scripta 14 (1979) 17-20

33. Cowley, J. M., High resolution studies of crystals using STEM, Chem. Scripta 14 (1979) 33-38

34. Wall, J. S. Visibility of heavy atoms, Chem. Scripta 14 (1979) 271-278

35. Dexpert, H., Freund, E., Lynch, J., Characterisation of supported metallic catalysts in a STEM, Proc. Metals Soc. Conf. (Inst. of Physics, London 1981) to appear

36. Fisher, R. M., Smith, D. J., Freeman, L. A. Pennycook, S. J. and Howie, A., Electron optical characterisation of graphimets, Carbon Conf. 14 (1979) 318

37. Batson, P. E., Damping of bulk plasmons in small Al spheres, Solid State Comm. 34 (1980) 477-480

38. Osakabe, N., Tanishiro, Y., Yagi, K. and Honjo, G. Reflection E.M. of clean and Au deposited (111) Si surfaces, Surface Science 97 (1980) 393-408

39. Turner, P. S. and Cowley, J. M., Bragg and Laue-Bragg waves, Ultramicrosc. 6 (1981) 125-138

40. Wells, O. C., Low loss images for surface scanning electron microscopy, Appl. Phys. Lett. 19 (1971) 232-235

41. Treacy, M. M. J., Krakow, W., Smith, D. A. and Trafas, G., A technique for comparing the bulk and surface structures of defects in thin films in the STEM, Appl. Phys. Lett. 39 (1981) 341-343

42. Morin, P., Pitaval, M., Besnard, D. and Fontaine, G., Electron channelling imaging in SEM, Phil. Mag. 40A (1979) 511-524

43. Venables, J. A., Electron microscopy of surfaces, Ultramicroscopy (1981) to appear.